




The 30 October 2020 Aegean Sea Tsunami: Post-Event Field Survey Along Turkish Coast

GOZDE GUNEY DOGAN,¹  AHMET CEVDET YALCINER,¹ YALCIN YUKSEL,² ERGIN ULUTAŞ,³ ORHAN POLAT,⁴
IŞIKHAN GÜLER,¹ CIHAN ŞAHİN,² AHMET TARIH,⁵ and UTKU KÂNOĞLU⁶

Abstract—On 30 October 2020, a strong normal-faulting earthquake struck Samos Island in Greece and İzmir Province in Turkey, both in the eastern Aegean Sea. The earthquake generated a tsunami that hit the coasts of Samos Island, Greece and İzmir, Turkey. National teams performed two post-tsunami field surveys on 31 October to 1 November 2020, and 4–6 November 2020, along the Turkish coastline; while the former was a quick survey on the days following the tsunami, the latter involved more detailed measurement and investigation focusing on a ~ 110 -km-long coastline extending from Alaçatı (Çeşme District of İzmir) to Gümüldür (Menderes District of İzmir). The survey teams measured runup and tsunami heights, flow depths, and inundation distances at more than 120 points at eight different localities. The largest tsunami runup among the surveyed locations was measured as 3.8 m in Akarca at a distance of 91 m from the shoreline. The maximum tsunami height of 2.3 m (with a flow depth of 1.4 m) was observed at Kaleiçi region in Sığacık, where the most severe tsunami damage was observed. There, the maximum runup height was measured as 1.9 m at the northeastern side of the bay. The survey team also investigated tsunami damage to coastal structures, noticing a gradual decrease in the impact from Gümüldür to further southeast. The findings of this field survey provide insights into the coastal impact of local tsunamis in the Aegean Sea.

Keywords: Tsunami, post-tsunami survey, runup, tsunami height, flow depth, inundation, coastal damage, Samos, Sığacık, Seferihisar, Aegean Sea.

1. Introduction

Mediterranean communities tend to settle in low-lying coastal zones, prone to marine hazards, including tsunamis. This rapid demographic growth, often accompanied by extensive economic activities, drastically increases the coastal community's exposure to tsunamis. In the Aegean Sea, the densely populated coastal areas have been exposed to several tsunamis in the past, some being devastating (Altınok and Ersoy 2000; Altınok et al. 2011; Ambraseys 1962; Ambraseys and Synolakis 2010; Dominey-Howes 2002; Galanopoulos 1960; Kuran and Yalciner 1993; Minoura et al. 2000; Papadopoulos and Chalkis 1984; Papadopoulos et al. 2014; Tinti et al. 2001). The most well-known tsunami in the region is the 1956 Amorgos event (M_w 7.8) that caused runup heights up to 25 m (Beisel et al. 2009; Okal et al. 2009; Papadopoulos and Pavlides 1992; Papazachos et al. 1985; Yalciner et al. 1995). More recently, the eastern Aegean Sea was the place of two tsunamis that followed M_w 6.3 and 6.6 magnitude earthquakes in June and July 2017, respectively. Both the 12 June 2017 Lesvos and the 21 July 2017 Bodrum–Kos events brought to the fore the tsunami threat from moderate magnitude earthquakes in the region, serving as reminders to the coastal communities. The latter event caused a significant impact on the southern coast of Bodrum Peninsula in Turkey and Kos Port in Kos Island in Greece (Dogan et al. 2019).

İzmir Metropolitan City, located at the western extremity of Turkey, has a ~ 629 -km-long coastline in the eastern Aegean Sea and is the third largest city in the country in terms of population, industrial density, capacity, and contribution to the national economy, following İstanbul and Ankara. Here, tsunamis were documented in the past after the

¹ Ocean Engineering Research Center, Department of Civil Engineering, Middle East Technical University, Ankara, Turkey. E-mail: gguneodyogan@gmail.com

² Hydraulics Division, Department of Civil Engineering, Yıldız Technical University, İstanbul, Turkey.

³ Seismology Division, Department of Geophysics Engineering, Kocaeli University, Kocaeli, Turkey.

⁴ Seismology Division, Department of Geophysics Engineering, Dokuz Eylül University, İzmir, Turkey.

⁵ Directorate of Earthquake and Ground Research, İstanbul Metropolitan Municipality, İstanbul, Turkey.

⁶ Department of Engineering Sciences, Middle East Technical University, Ankara, Turkey.

earthquakes of 20 March 1389 in Chios, Greece, 10 July 1688 in İzmir Bay, Turkey, and 12 May and 8 September 1852 in İzmir (Altınok and Ersoy 2000; Altınok et al. 2011). Specifically, the 3 April 1881 Chios earthquake (M_w 6.5) generated a tsunami affecting the Çeşme coast with a Medvedev–Sponheuer–Karnik (MSK) (Sponheuer and Karnik 1964) intensity $I_0 = 9$ in some residential areas (Altınok et al. 2005).

On 30 October 2020, a strong normal-faulting earthquake (M_w 6.6, AFAD 2020) struck Samos Island in Greece and İzmir Province in Turkey in the eastern Aegean. The tsunami that followed the earthquake caused significant damage in Çeşme and Seferihisar Districts of İzmir and Samos Island coasts, and resulted in one casualty and several injured people from the tsunami on the Turkish side (Anadolu Agency 2020). Kandilli Observatory and Earthquake Research Institute (KOERI), Turkey's national tsunami warning center and tsunami service provider for the North-Eastern Atlantic, the Mediterranean and Connected Seas Tsunami Warning System (NEAMTWS), issued a tsunami warning 11 min after the main event.

We present the results from the two field surveys conducted by national teams along the Aegean coast of Turkey to collect the tsunami data following the 30 October 2020 Samos–İzmir event. Our results include flow depth, runup and inundation measurements, arrival time, and coastal damage observations. Furthermore, we discuss the survey findings to better understand the tsunami behavior and its effects on the nearby coastal areas.

2. Seismotectonics

The eastern Aegean Sea region is characterized predominantly by dip-slip extensional tectonics (Aktar et al. 2007; Jackson 1994; Taymaz et al. 1991). It includes E–W trending faults by the areas extending in N–S direction and exhibits dextral (right-lateral) or sinistral (left-lateral) components (Dewey and Şengör 1979; Jackson and McKenzie 1988; Taymaz et al. 1991; Papazachos et al. 1998; Bozkurt 2003; Emre et al. 2011; Tan et al. 2014; Tepe and Sözbilir 2017). Therefore, the tsunami

threat in the study area is mainly associated with dominant normal faults that reveal a high potential risk for coastal areas.

On 30 October 2020, 12:51 UTC (14:51 local time), a submarine earthquake (M_w 6.6) occurred at the north of Samos Island, Greece, and offshore Seferihisar–İzmir, Turkey, with an epicenter of (37.88° N, 26.70° E) at a depth of ~ 15 km (AFAD 2020). A total of 39 foreshocks occurred in the epicenter's vicinity within the last 3 months before the event. Magnitudes of these earthquakes were not significant except the one with a magnitude of M_w 3.6 that occurred approximately at a 7 km depth on 9 October 2020, about 5 km west of the mainshock (Fig. 1).

More than 4600 aftershocks have occurred by the end of November 2020, 50 having magnitudes $M_w \geq 4.0$. The largest one with a magnitude of M_w 5.1 occurred at 16:14 (UTC), about 4 h after the earthquake, approximately 10 km southeast of the epicenter at a depth of about 7 km. From the conjugate-type aftershocks distribution between Dilek Peninsula (DP) in Turkey and north of Ikaria Island of Greece, approximately 80–100 km rupture length in E–W direction is evident in four segments with visible seismic gaps. Three segments are located in the northern part of the Samos, while the eastern swarm is aligned on the NNE–SSW direction, which is parallel with the alignment of Büyük Menderes Graben (BMG) (Fig. 1). North of Kuşadası Bay (KB) and the western part of the Samos reveals diffuse-type seismic activity. Nevertheless, a clear local cluster is prominent near Orhanlı–Tuzla Fault (OTF) between Gümlüdür and Özdere Districts (Fig. 1). The present state of the aftershock distributions points to conjugate faulting as suggested by Aktar et al. (2007) for the earthquake swarm (M_w 5.9) on 17–21 October 2005 in Sığacık Bay (SB).

The fault plane solution of the mainshock shows a normal fault rupture on an E–W aligned plane dipping $\sim 40^\circ$ to the north, according to the preliminary results of AFAD. All other focal mechanism solutions obtained from aftershocks also indicate dip-slip (dominant normal) faults with dip angles ranging from 33° to 74° towards the N or NE (Appendix 1 Table 1).

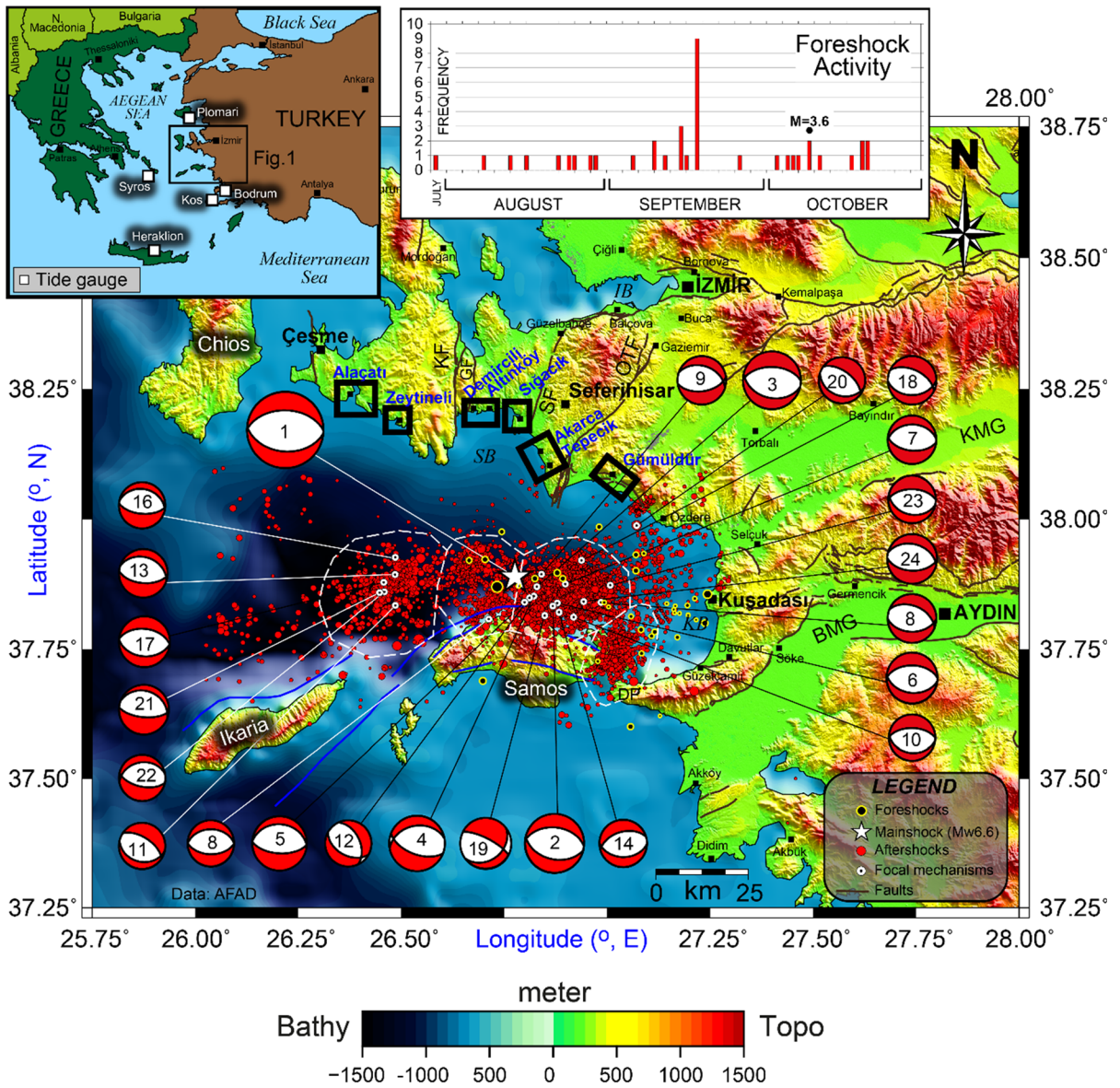


Figure 1

Seismotectonic map of Samos Island and its surroundings. The star shows the mainshock of 30 October 2020 Samos Island–İzmir earthquake (M_w 6.6). The beach balls present the focal mechanisms of the mainshock and the aftershocks given in Appendix 1, Table 1. The black and red circles indicate 3-month foreshocks and 2-month aftershocks, respectively, as of Ministry of Interior Disaster and Emergency Management of Presidency (AFAD 2020) data. Marine and terrestrial faults are compiled from Chatzipetros et al. (2013), Emre et al. (2013), Evelpidou et al. (2019), and Ring et al. (2017). The kinematic parameters of the focal mechanism solutions are given in Appendix 1, Table 1. (BMG Büyük Menderes Graben, DP Dilek Peninsula, GF Gülbahçe Fault, IB İzmir Bay, KF Karaburun Fault, KMG Küçük Menderes Graben, KB Kuşadası Bay, OTF Orhanlı-Tuzla Fault, SF Seferihisar Fault, SB Sığacık Bay). Black rectangles denote the post-tsunami survey localities. White rectangles represent tide gauges in the inset map. Bathymetric and topographic data are from EMODnet Digital Terrain Model (<https://www.emodnet-bathymetry.eu>)

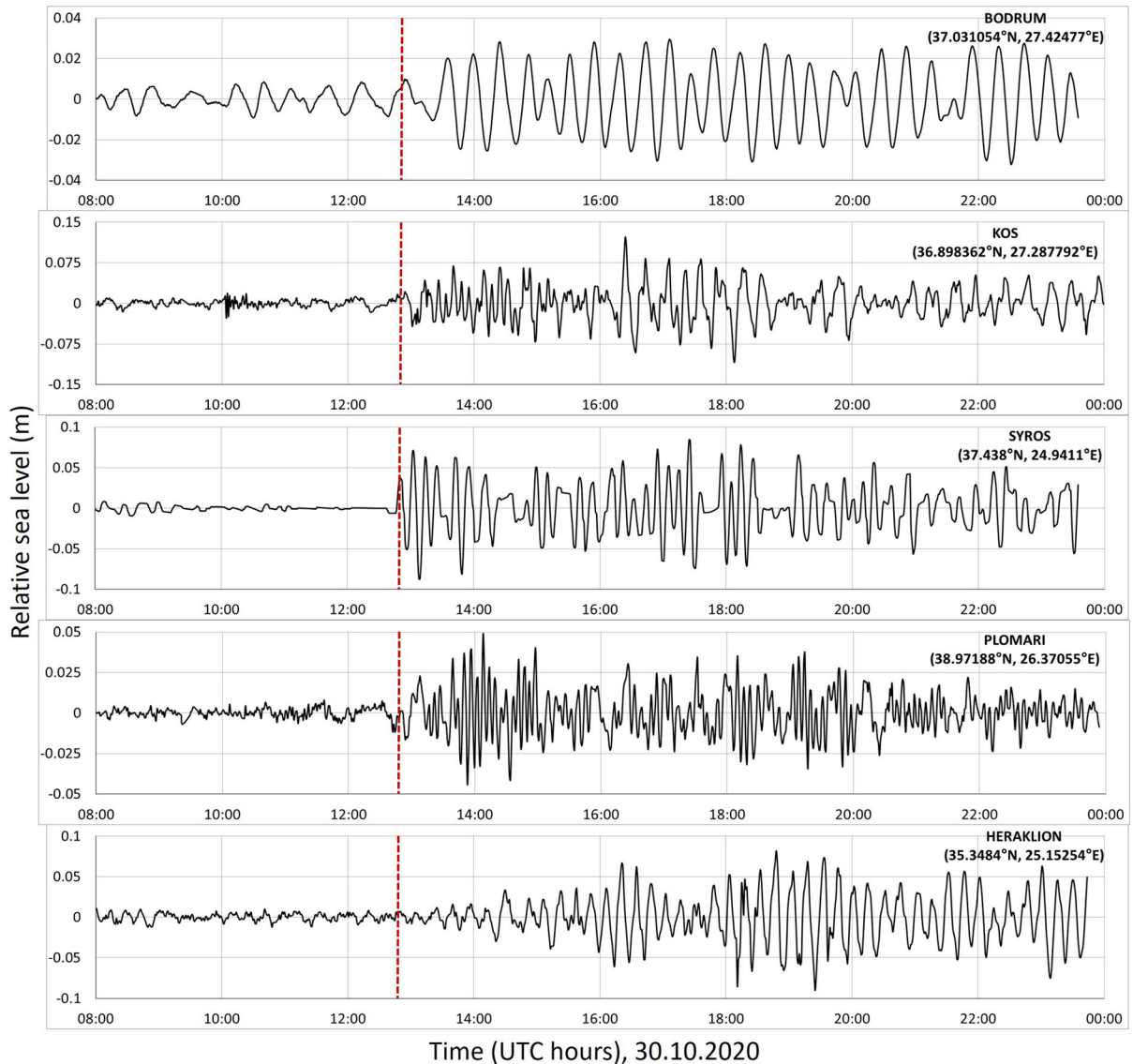


Figure 2

Detided tide-gauge measurements of five stations in the Aegean Sea for the 30 October 2020 tsunami. The red dashed lines show the earthquake time, 12:51 UTC

3. Sea-Level Recordings

The 30 October 2020 tsunami was recorded by the tide gauge network of the Aegean Sea (Fig. 1). However, as the sea level sensors are located outside the area majorly affected by the tsunami, none of the stations recorded sizable waves (Fig. 1). We present the detided measurements from five tide gauges (Fig. 2). The mareogram data recorded at 1 min

sampling intervals have been downloaded (<http://www.ioc-sealevelmonitoring.org/station.php?code=stationcode>), and the detiding process is carried out by using a fast Fourier transform (FFT) band-pass filter to remove the astronomical tide. There is a clear indication of the tsunami at all five stations. However, the measured amplitudes, ranging between 3 cm measured at Bodrum and 12 cm measured at Kos

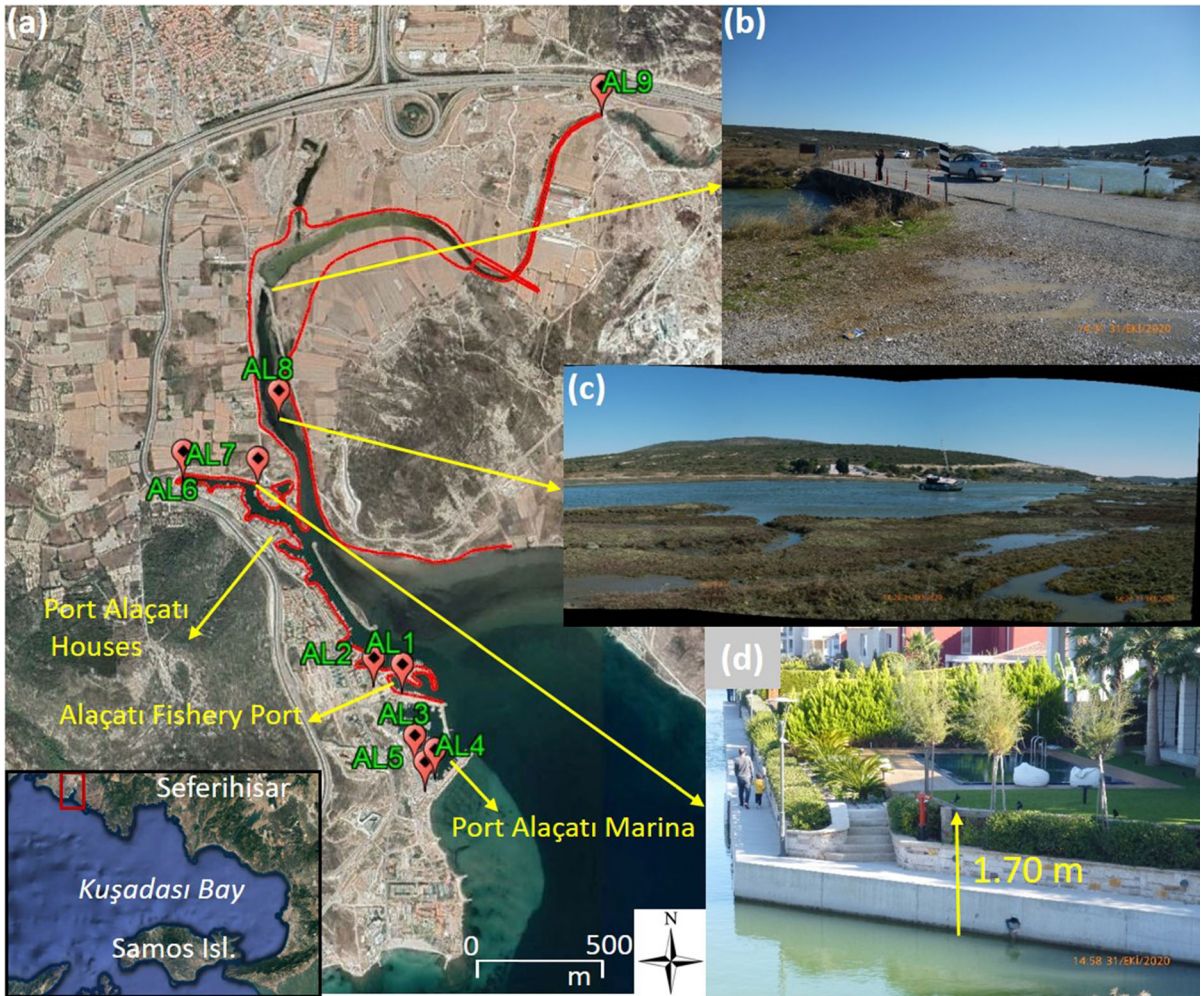


Figure 3

a Map showing the surveyed locations in Alaçatı locality (image is taken from Google Earth) The red line shows the tsunami penetration/inundation zone. **b** Tsunami traces visible on Alaçatı Azmak bridge (at ~ 30 cm above the bottom of the bridge wall) located 1.0 km away from the coastline (38.2706° N, 26.3768° E), **c** Fisher boat dragged 1160 m away from the fishery port along Alaçatı Azmak, **d** Water level increase at the garden wall of Alaçatı Port houses according to the house owner

station, are much smaller than the near-field observations, as can be expected from the gauge locations.

4. Post-tsunami Field Measurements

The main objectives of the post-tsunami field survey were (1) to document the tsunami effects along the coast, (2) to obtain any available data on the observed coastal amplitudes and inundation extent, (3) to perform audiovisual recording before cleanup, (4) to interview the eyewitnesses, and (5) to

understand and explain the event in detail. The first survey took place 2 days after the earthquake (31 October to 1 November 2020) to acquire data before any cleanup. The second survey was carried out on 4–6 November 2020, for a more detailed investigation, including flow depth, runup and inundation measurements, eyewitness accounts, and identification of damages to coastal structures. The tsunami characteristics were measured using the conventional methods described in the UNESCO-IOC ITST Post-Tsunami Survey Field Guide 2nd Edition (UNESCO-ITST 2014).



Figure 4

a Map showing the surveyed locations and the tsunami inundation zone (red line) in Zeytineli (image is taken from Google Earth). The corresponding survey location IDs are indicated at the lower left corner of each figure. **b** Damaged bridge on Zeytineli Azmak due to tsunami. **c** Panoramic view of tsunami inundation in Zeytineli. **d** Debris accumulated inside and at **e** outer wall of a house (flow depth 1.5 m). **f** Wave traces on palm tree near the coastline (flow depth 1.9 m)

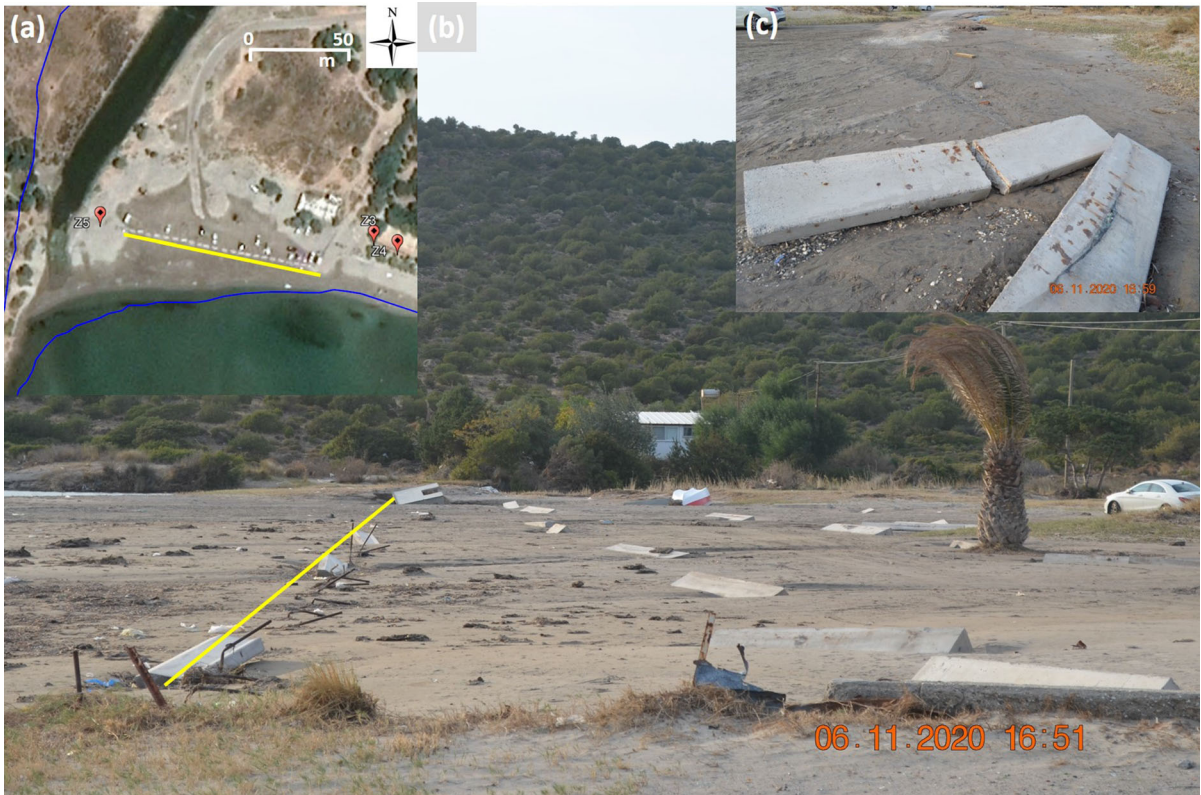


Figure 5

a Original layout of the concrete blocks in Zeytineli (image is taken from Google Earth). **b** Concrete blocks drifted and scattered by the tsunami. **c** Closer view of drifted and damaged concrete blocks. Yellow lines indicate the original location of the blocks before the tsunami

The survey covered the ~ 110 -km-long coastline and mainly focused on three regions (Fig. 1): (1) Alaçatı and Zeytineli on the northwestern coast, (2) Demircili, Altıncöy, Sığacık, Akarca, and Tepecik in the Seferihisar District on the northern coast, and (3) Gümüldür on the northeastern coast with respect to the earthquake epicenter. The teams collected field data on tsunami penetration evidence such as deposited debris, watermarks left on structures, and damage to vegetation and objects. We conducted eyewitness interviews and gathered available video recordings to obtain more information on the tsunami behavior at the time of the event. Laser ruler instruments and two GPS stations (ProMark 700) were used to perform flow depth, runup, and inundation measurements. All measurements were then referenced to the sea level at the time of the event, which was at low tide, 0.2 m, with respect to the mean lower low water (MLLW) (<http://tides4fishing.com/as/>

[turkey/izmir](http://tides4fishing.com/as/turkey/izmir)). This level was determined according to the long-term water level marks at the quay walls of Port Alaçatı and Sığacık Marinas, also confirmed by the managers of these marinas (assuming no significant variations in the sea level inside the marinas). The results of the survey are summarized in Appendix 2, Table 1.

4.1. Observations in the North-Western Coast

4.1.1 Alaçatı Locality

In Alaçatı, there is a stream—*azmak* in Turkish—called Alaçatı Azmak where maximum tsunami penetration was ~ 2490 m (Fig. 3a, Table 2-AL9). The tsunami inundation mainly followed the *azmak* streambed and the flat coastal topography (Fig. 3a). A boat was dragged ~ 1160 m along the stream (Fig. 3a–c, Table 2-AL8) from its location in the

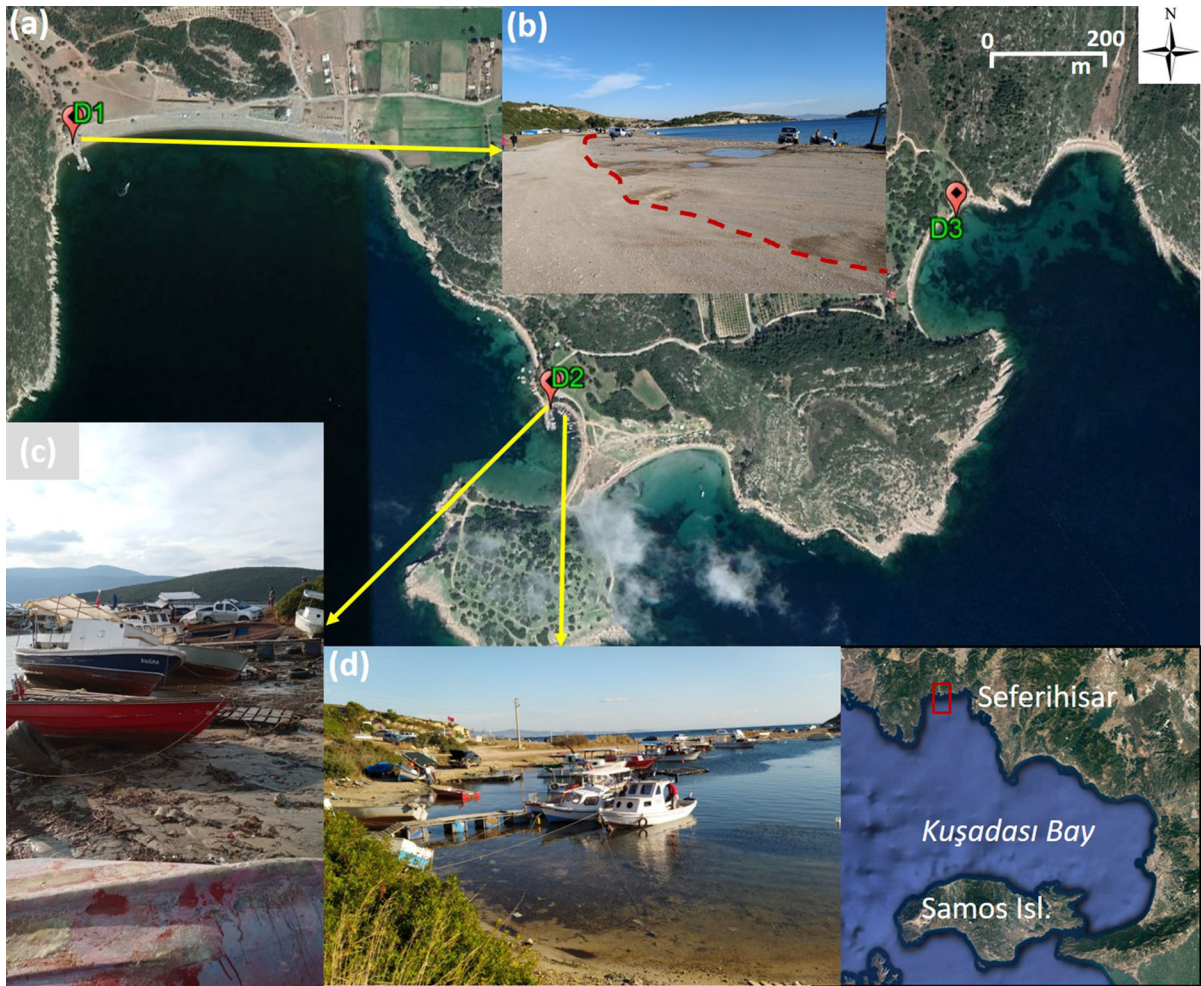


Figure 6

a Map showing the surveyed locations in Demircili (image is taken from Google Earth). **b** Small tsunami inundation (red line) in Demircili Beach on the northwestern side of the bay **c, d** Damaged boats observed in the small fishery structure on the southeastern bay of Demircili

fishery port. In the fishery port and Port Alaçatı Marina, the maximum inundation distances were ~ 73 m with runup heights of around 1.0 m (Fig. 3, Table 2-AL2 and AL5). According to house owners and video recordings, Port Alaçatı houses were also affected by the tsunami, where the water level rose by 1.7 m (Fig. 3d, Table 2-AL6 and AL7). According to the Port Alaçatı houses manager, before the first positive wave arrived, the sea receded to a depth of 1.5 m, 28 min after the earthquake, confirmed by security video recordings (Appendix 3, Fig. 21).

4.1.2 Zeytineli Locality

Zeytineli was the area most impacted by the tsunami on the northwestern coastline (to the epicenter), where a significant tsunami penetration was observed along the stream, Zeytineli Azmak. The tsunami inundation zone mainly followed the streambed and the surrounding low-lying flat topography, as there are steep slopes on both sides (mountainside) (Fig. 4a–c). The abandoned summerhouses along the shore were severely damaged, and debris accumulated on both outer walls and inside (Fig. 4d–e, Table 2-Z3 and Z4). The maximum inundation distance was ~ 760 m along the NNE–SSW

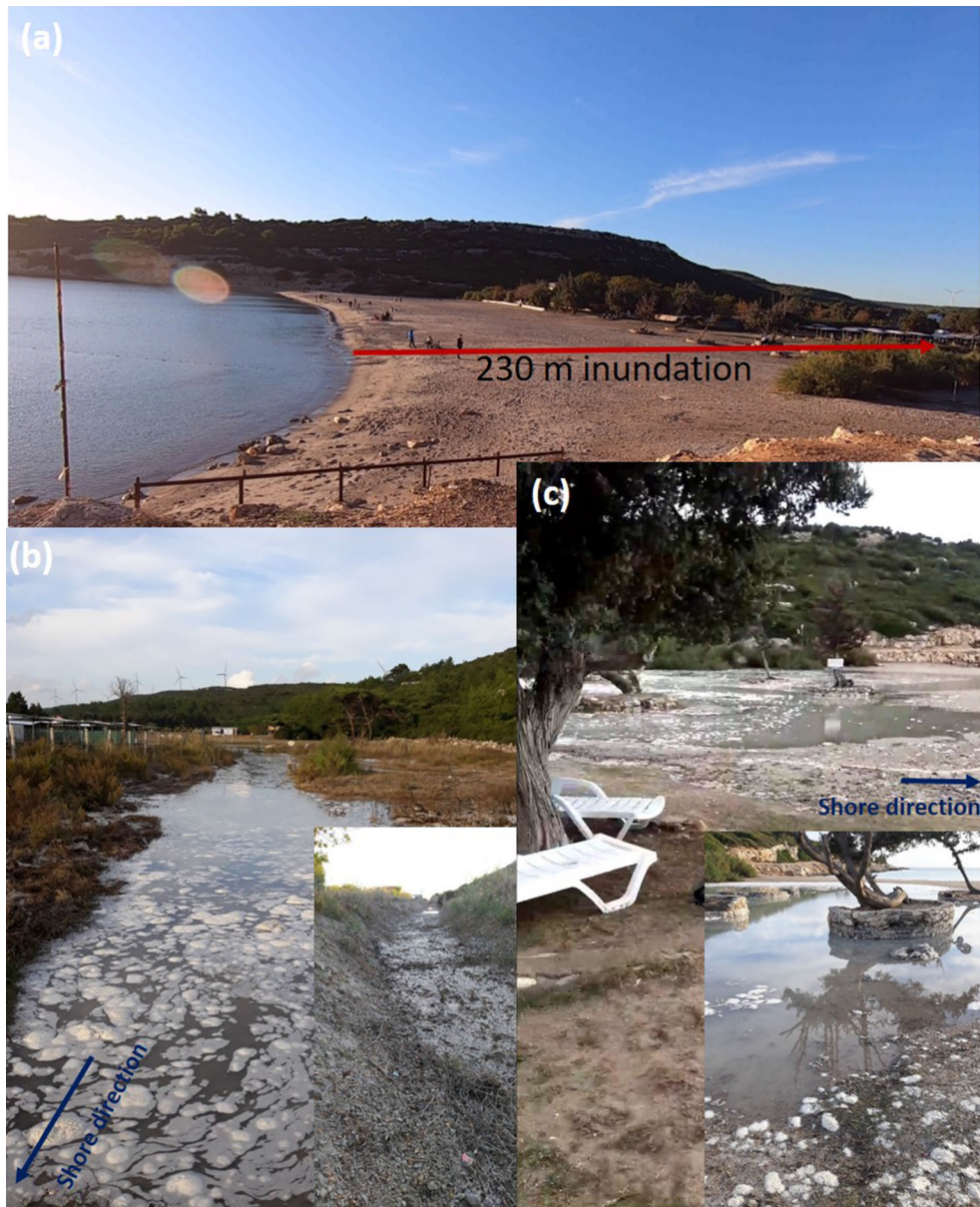


Figure 7

a Tsunami inundation area in Altinköy locality **a** on the beach, **b** along the streambed, and **c** on the beach in closer view (photos in insets (**b**, **c**) were provided by eyewitnesses)

direction from the sea coast. The flow depth was 1.9 m on the palm trees, 50 m away from the coastline (Fig. 4f, Table 2-Z5). Additionally, concrete blocks ($30 \times 50 \times 300$ cm), weighing approximately 1 ton, were found dragged 20–25 m inland direction and scattered from their original locations by the tsunami (Fig. 5).

4.2. Observations in the Northern Coast

4.2.1 Demircili and Altinköy Localities

The tsunami impact was quite different in the northwestern and southeastern parts of the coastline in Demircili. Only a small inundation of ~ 45 m was measured on the northwestern side of the coast



Figure 8

General view of the surveyed locations in Siğacık. Dashed yellow lines show the local river/riverbeds where the tsunami penetrated. Teos Marina and Kaleiçi regions experienced heavy damage. There was significant inundation in the most low-lying area (~ 410 m) due to an incoming wave through the bay (Table 2-S19) as well as through Teos Marina (Table 2-S30) (image is taken from Google Earth)

(Fig. 6, Table 2-D1). On the other hand, considerable damage was observed by the local people and fishers on a narrow beach on the southeastern side of the bay

(Fig. 6, Table 2-D2). According to eyewitnesses, the sea receded almost 20 min after the earthquake and returned in 3–4 min. They observed this receding–

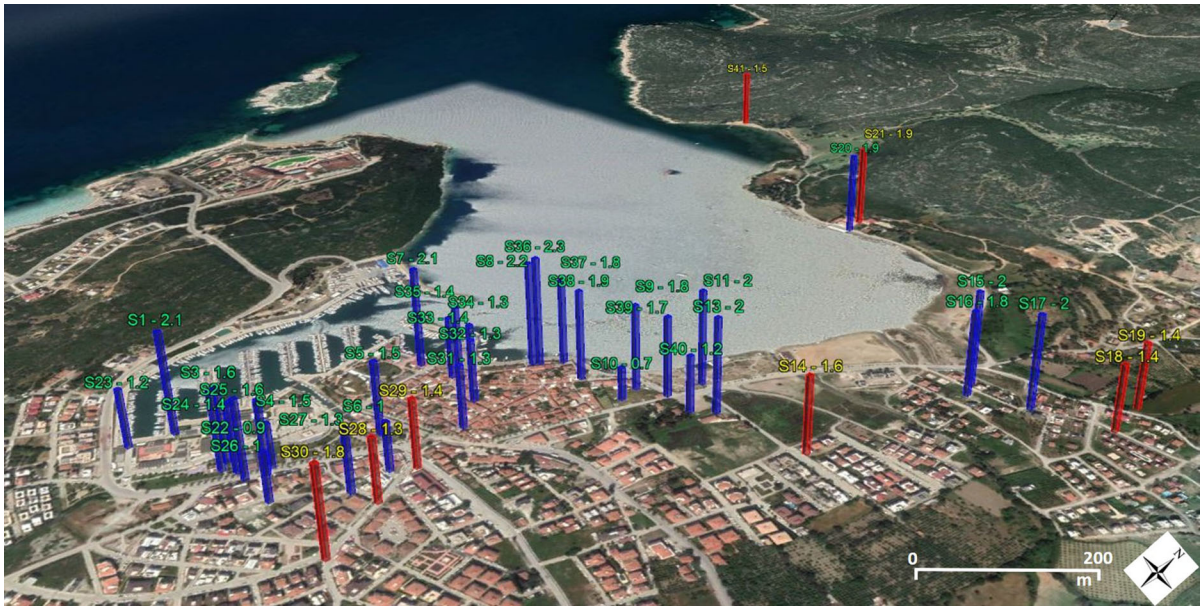


Figure 9

Distribution of the measured tsunami and runup heights along the surveyed coastline in Siğacık due to the 30 October 2020 tsunami. The blue bars represent the tsunami height, and the red ones represent the runup. The labels are given as survey point ID–measured value (m)

inundation for almost 5 h. Boats moored at a depth of 1.8 m were grounded when the sea receded. Here, the water level rose by more than 1 m inside the small fishery shelter. Further east, the runup was 0.7 m on Denizyıldızı beach (Fig. 6, Table 2-D3), and the inundation distance was about 15 m at this location, as inferred from seaweed deposits.

In Altıncöy, the tsunami inundated the beach up to ~ 230 m (Fig. 7a, Table 2-ALT1). The tsunami penetration along the streambed reached ~ 600 m with a flow depth of 0.2 m (Fig. 7b, Table 2-ALT2).

4.2.2 Siğacık Locality

Siğacık, a low-lying bay-shaped area with several local streambeds, was the most impacted area of the tsunami-affected coastline (Fig. 8). The tsunami height measurements at surveyed locations in Siğacık range from 0.9 to 2.3 m (Fig. 9). We measured the maximum runup as 1.9 m (Table 2-S21). Further tsunami inundation and impact were observed in the low-lying areas surrounding the local streams of the bay (Figs. 8, 9). We observed significant inundation in the most low-lying area (Fig. 8). Here, we measured the inundation distance as ~ 410 m

(Table 2-S19). The tsunami also caused significant damage to properties and houses at that location, leaving injured locals who barely survived the tsunami (Fig. 10a–d).

In Teos Ancient City, which was one of the 12 Ionian city-states established on the coast of the Aegean Sea in Western Anatolia, two ports were serving the city, the southern port with an entrance 8 km south of Siğacık and the northern port located near Siğacık, at the location of the current Teos Marina. We found inland tsunami traces at a distance of ~ 550 m from the shore, penetrated along the low-lying old streambed area, which was connecting the ancient city to the sea. The tsunami completely inundated the southern port facilities (storage buildings, service structures, and berthing places) of Teos Ancient City.

We observed significant damage in Teos Marina, one of the significant coastal facilities (for more information, see Sect. 5). The flow depth was measured as 0.9 m on the garden fence of the port near the pedestrian entrance, corresponding to a tsunami height of 2.1 m (Fig. 11a, Table 2-S1). The tsunami penetrated ~ 210 m through a local stream



Figure 10

Observed damage on garden walls and summerhouse garden entrances at low-lying maximum inundation area in Sığacık locality **a–c** at point S16, **d** at point S15

connected to the sea inside the marina and flooded the surrounding area with a flow depth of 0.5 m (1.5 m in the streambed) (Fig. 11b, Table 2-S5). At another local stream, further northeast from Teos Marina, the tsunami penetration caused a 1.5 m water level rise from the streambed ground overflowing the small bridge at the upstream, according to eyewitnesses (Table 2-S11). Figure 11c shows damaged boats and seafront facilities on the Sığacık coastline.

Kaleiçi region, located along the coastline with many cafes and shops, was heavily damaged (Fig. 12a–e). We examined the incoming tsunami dynamics in Kaleiçi from a security video recording (Appendix 3 Fig. 22). According to our inferences, the maximum sea withdrawal occurred ~ 13 min after the earthquake, while the first positive wave arrived at ~ 18 min.

4.2.3 Akarca Locality

The Akarca coast has three bays, with a highly localized tsunami impact in the central one and a significant reduction in the northwest and southeast directions (Fig. 13a, Table 2-A30, A32, A36–A40). We collected a significant number of measurements in the central part of Akarca and gathered information from eyewitnesses. The maximum inundation distance in Akarca was measured as ~ 290 m (Fig. 13b, Table 2-A8). We present two different cross-sectional profiles of tsunami height measurements in Fig. 13c–d. The tsunami height and runup distributions along the surveyed coastline are also given in Fig. 14. The maximum runup among all surveyed locations was measured as 3.8 m (Fig. 15a, Table 2-A5) and observed at a distance of 91 m from the shore.



Figure 11

a Tsunami traces on the garden fence of Teos Marina (S1) corresponding to a flow depth of 0.9 m. **b** Tsunami flood traces on the iron fences of a local river, connected to the sea inside Teos Marina, found at ~ 210 m inland with a flow depth of 0.5 m (1.5 m in the riverbed). **c** Damaged boats and seafront facilities on Sığacık coastline

Seferihisar Diving Center, located in the central part of Akarca, was severely damaged by the tsunami with a flow depth of 2.2 m (Fig. 15b, Table 2-A24). Here, the sea receded ~ 180 m to a depth of ~ 4 m. The diving center owner stated that he was drifted by the incoming wave to 200–250 m inland on a sofa and barely survived the tsunami. The inundation distance here reached 280 m. He described the first wave's arrival time as 10–12 min after the earthquake, observing four to five waves with 8–10 min between successive waves.

The garden fences and walls of the shore-facing summer houses also had notable damage (Fig. 15c–d, Table 2-A15). We measured 1.9 m splash height on a vertical wall of a house located just near the shore (Fig. 15c, Table 2-A1). A boat was dragged 90 m inland by the tsunami (Fig. 16a, Table 2-A6), where a car (~ 55 m) and a water storage tank (half full) were also dragged inland by the strong waves (Fig. 16b–d, Table 2-A3).

4.2.4 Tepecik Locality

Tepecik is another region where we noticed localized tsunami effects in several small bay-shaped areas. There was an overall decrease in the tsunami impact here compared with Akarca, with continuing impact decrease to the southeastern direction. The highland topography of this coastal area and the absence of many streams/streambeds (except one location, Table 2-T3) might be the reasons. Only small inundation was observed according to deposits on

the beaches (Fig. 17a–b, Table 2-T1 and T5). The local maximum inundation reached 120 m along a small stream (Table 2-T3), where inundation was 20 m on the beach (Table 2-T2). A flow depth of 1.5 m was measured at location Table 2-T4, where the ground elevation was ~ 0.5 m above the sea level.

4.3. Observations in the Northeastern Coast

4.3.1 Gümüldür Locality

Minor tsunami impact was observed in Gümüldür, mainly limited to narrow beach areas. The inundation distances ranged between 15 m and 25 m (Table 2-G1–G6), with a maximum value measured at the beach in front of Rafael Boutique Hotel (Table 2-G1). We found tsunami trace on a small pier with a flow depth of 0.5 m at only one location in Gümüldür (Table 2-G4).

We acquired information from local eyewitnesses about the tsunami behavior in Davutlar in Kuşadası District, the most southeastern coast from the epicenter. According to eyewitnesses, there was no significant abnormal water surface fluctuation or inundation in Davutlar. The tsunami penetrated ~ 30 m along a small streambed in Sevgi Beach in Davutlar. Our field observations show a significant reduction in the coastal impacts east from the V-shaped cape between Tepecik and Gümüldür.



Figure 12

Heavily damaged cafes and shops in Kaleiçi region in Siğacık locality at points a S9, b S43, c S4, d, and e S9–S10

5. Observations of Tsunami Dynamics and Impact/ Damage on Coastal Facilities

In addition to the measurements of coastal tsunami parameters, we investigated the tsunami impact on coastal facilities, including small fishery shelters, ports, and marinas. Most of the damaged structures were poorly engineered structures, except Teos Marina in Siğacık. Teos Marina is a modern five-anchor quality marina, constructed and operated according to the national and international engineering and operational standards with 560 boat capacity.

In Teos Marina (Fig. 8), four piers out of six (composed of floating pontoons) were displaced, and more than 320 boats were moved (some boats sank, and some were moved outside the marina by the tsunami). Figure 18 shows the Teos Marina's layout and the boats before (Fig. 18a) and after (Fig. 18b–c) the tsunami. There is a stream inside the marina (Fig. 8) through which the tsunami penetrated and inundated Siğacık town. The backflow of inundation through the local stream discharging to the marina basin seems to be the primary cause of the strong currents and associated damage in Teos Marina.

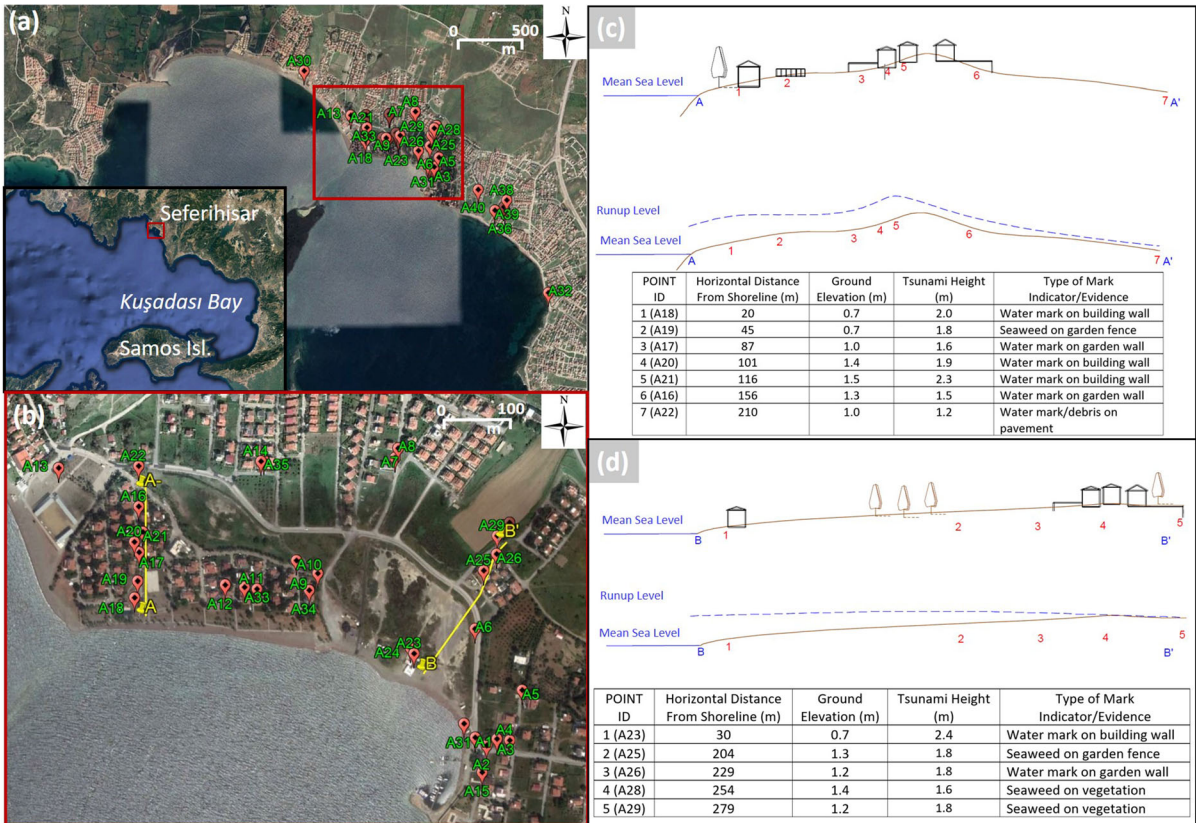


Figure 13

a General and **b** closer view of the surveyed locations in Akarca. The red rectangle shows the central bay of Akarca, where the tsunami impact was highly localized. **c, d** Cross profiles of measured tsunami inundation heights in Akarca at A–A' and B–B', respectively (image is taken from Google Earth)

According to the general manager, the marina experienced large period oscillations lasting 4–5 h with an amplitude of 0.7 m. He stated that, 15 min after the earthquake, the marina's water level decreased until the sea bottom appeared at some parts. Eyewitnesses heard loud bursts due to the breaking of the ropes connecting boats to the pontoons. Some boats were grounded on the sea bottom. Twenty minutes after the earthquake, the incoming waves caused strong current speeds and eddies inside the marina. The water level increased and reached ~ 2 m above the mean sea level at fixed berthing places ~ 25 min after the earthquake. He also informed that the second wave was more destructive, causing significant damage and grounding the boats to the sea bottom.

Port Alaçatı Marina (Fig. 3), which was well-engineered and floating concrete pontoons with 250

boat capacity, had damage only on connection points of the floating piers to the docks and fuel station, according to the general manager. However, considerable damage was reported in the fishery port located near the marina. The sea receded to a depth of ~ 2.5 m, 13 min after the earthquake, based on eyewitness interviews. The incoming wave was observed 20 min after the earthquake, 7–8 min after the withdrawal, and the water level rose to 1.5 m inside the marina.

The small fishery port in Akarca suffered substantial damage. All of the floating piers (Fig. 19a–b) and many port facilities (Fig. 19c–d) were destroyed and became unusable. More than 20 boats were sunk, as reported by the Akarca fishery cooperative president.

We also observed severe tsunami damage at another small fishery shelter in Zeytineli (Fig. 20).

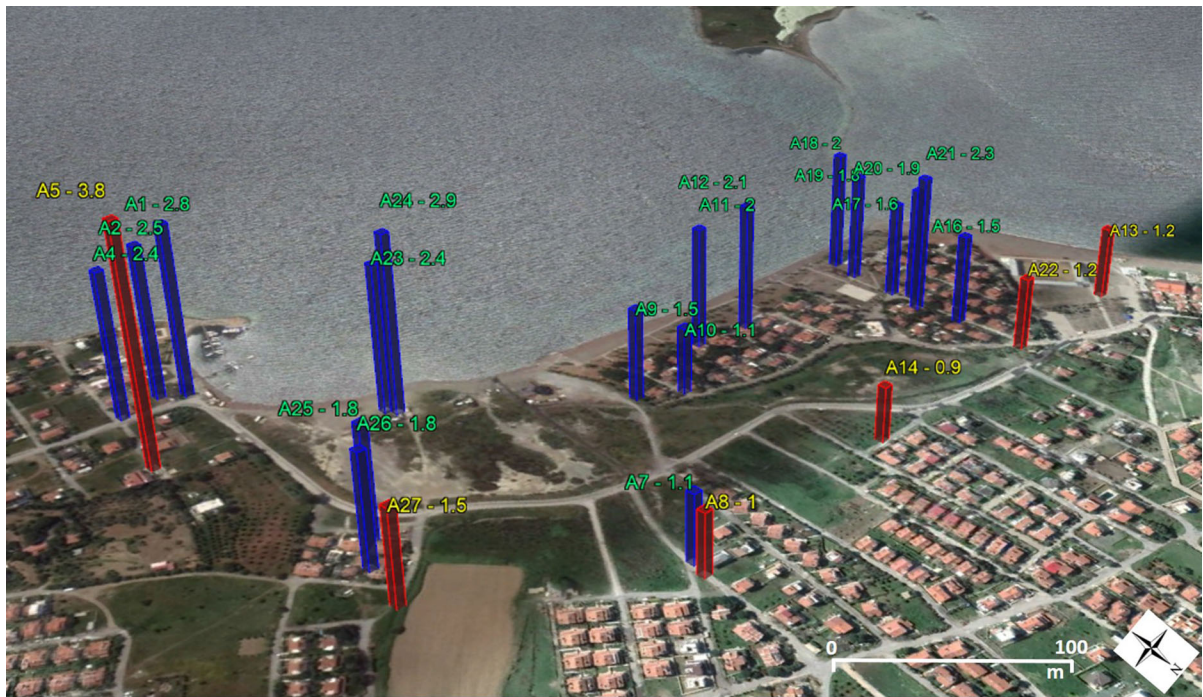


Figure 14

Distribution of the measured tsunami and runup heights along the surveyed coastline in Akarca. The blue bars represent the tsunami height, and the red ones represent the runup. The labels are given in a point ID–measured value format

The poorly engineered mooring and berthing structures and all of the boats in the shelter were destroyed and became unusable, requiring complete reconstruction. The cars parked close to the shore were drifted to the sea. The sunk boats were required rescue operations.

6. Discussion and Conclusions

The tsunami that followed the 30 October 2020 earthquake confirms the potential tsunami generation of segmented normal faults in the eastern Aegean and highlights the tsunami threat in the region. The results of the post-tsunami field surveys performed along a ~ 110-km-long coastline demonstrate the significant tsunami impact. This study's primary limitation was that the fieldwork had to be performed under Covid-19 pandemic conditions, limiting time and human interaction considerably. Nevertheless, we attempted to attain clear information based on evidence, which

necessitates a proper evaluation of the tsunami traces and eyewitness observations.

According to our findings from the field reconnaissances and eyewitness reports, the most impacted areas were Sığacık, especially Sığacık Teos Marina, and Akarca, about 30 km north from the epicenter. In Sığacık, the maximum inundation distance was measured as ~ 410 m, whereas it reached ~ 290 m in Akarca. Two hundred boats were sunk and destroyed at heavily damaged Teos Marina. In Teos Ancient City, located at the south of Sığacık, the inundation distance reached 550 m. The tsunami penetrated ~ 2490 m along Alaçatı Azmak (stream) and inundated the surrounding low-lying areas. The maximum inundation was ~ 760 m in Zeytineli, among all surveyed locations.

In the northwest, in Zeytineli, the local maximum flow depth was 1.9 m on the palm trees 50 m away from the coastline, whereas the local maximum runup reached 2.4 m. The maximum tsunami height was obtained in the Kaleiçi region of Sığacık and measured as 2.3 m, corresponding to a flow depth of



Figure 15

Observed destruction on properties and tsunami debris at summerhouse gardens in Akarca **a** tsunami deposits observed at maximum runup (3.8 m) (A5), **b** destruction in Seferihisar Diving Center where 2.2 m flow depth was measured (A24), **c** destroyed concrete garden walls of a summerhouse (A1) (1.9 m splash height measurement is shown on the upper-right inset), **d** destroyed iron garden fences of a summerhouse (A15)

1.4 m. The maximum tsunami runup of 3.8 m was measured at an inundation distance of 91 m at Akarca. The tsunami impact decreased dramatically after the “V” shaped peninsula between Tepecik and Gümüldür localities. We identified almost no significant inundation or other indications of tsunami impact beyond Gümüldür, southeast of the earthquake epicenter.

On the Greek side, the 30 October tsunami impacted the island of Samos within a few minutes. In the harbor of Karlovasi, located on the island’s NW side and one of the nearest coastal locations to the fault rupture area, wave runup reached 1.8 m. The most impacted area of Samos Island is its most populated town of Vathy, where a series of waves flooded the waterfront buildings. On the southern coast of Samos, wave runup reached 0.5 m, and the tsunami did not inundate the waterfront of the harbor in Pythagorion (Kalligeris, personal communication).

In Samos, a maximum inundation of 102 m was reported in Vathy town on the northeast coast (Triantafyllou et al. 2021).

To summarize, our findings reveal a significant amplification of the tsunami in small bays with narrow entrances, resulting in highly localized tsunami effects. The tsunami impact in such locations (especially in Sığacık and the central bay of Akarca) was much more severe than in other surveyed areas. The surveyed coastlines contain many streams (Azmak), which increased the potential tsunami inundation and impact. We also observed severe damage on properties at various surveyed locations, especially in poorly engineered coastal structures, i.e., fishery shelters.

An important survey finding was the remarkable level of tsunami awareness among the population of the surveyed coastlines. Most people moved away from the shores after noticing the sea withdrawal,



Figure 16

a A boat dragged 90 m inland in Akarca (A6). **b** Damaged shore-facing structures in Akarca fishery port area. **c** Half-full water storage tank (in red rectangles) dragged from the shoreline. **d** A car dragged 55 m inland and damaged by the tsunami at point A3

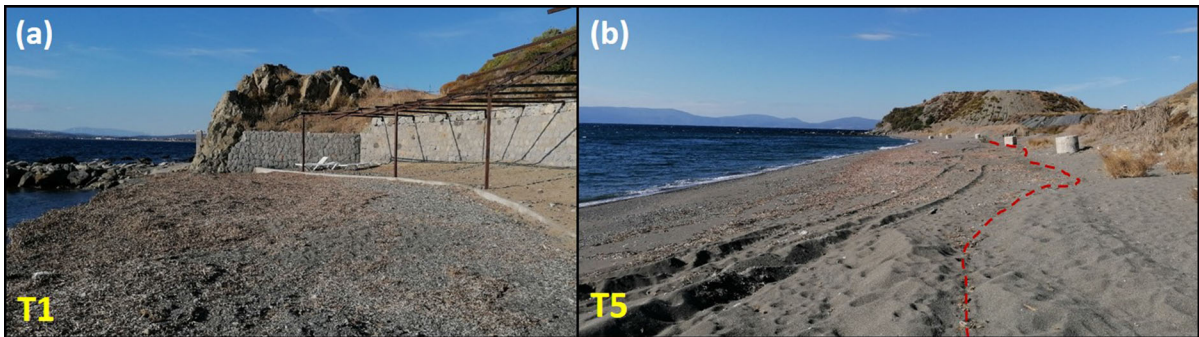


Figure 17

a Sweep deposits found at points **a** T1 and **b** T5 in Tepecik locality, where the tsunami inundation and impact was limited to these small inundation areas. The red dashed line indicates the estimated inundation border at point T5 according to the sweep deposits

which may be considered a successful self-evacuation. Unfortunately, an older woman was reported dead after failing to resist strong currents generated by the tsunami.

The eastern Aegean coastal settlements experienced three significant normal-faulting events in the

last decade, i.e., 12 June 2017 Lesvos-Karaburun (M_w 6.3) 20 July 2017 Bodrum-Kos (M_w 6.6), and 30 October 2020 Aegean Sea (M_w 6.6), generating tsunamis. The first two tsunami events occurred at approximately 110 km north–northwest and south–southeast from the 30 October earthquake's



Figure 18

View of Teos Marina layout **a** before and **b** after the event with damaged pontoons (taken from a local newspaper, <https://www.sabah.com.tr/video/yasam/depremin-merkez-ussu-seferisar-sigaciktaki-tsunami-felaketi-havadan-boyle-goruntulendi-video>), and **c** after the event taken by a drone showing the damaged pontoons and boats (provided by a boat owner in the marina)



Figure 19

Observed damage in **a**, **b** the floating piers used for berthing and mooring, and **c**, **d** the seafront harbor facilities in Akarca fishery shelter



Figure 20

Photos showing heavy damage in Zeytineli fishery shelter where all of the boats and mooring facilities were unusable after the tsunami

epicenter. The former event caused only minor impact with observed coastal amplitudes less than 0.5 m in Plomari town and surrounding areas in Greece, and Karaburun and Foça towns in Turkey. The second event, the Bodrum-Kos tsunami, resulted in a more remarkable impact with significant boat and property damage in Bodrum Peninsula, Turkey, and Kos Island, Greece, showing similarities with the latest tsunami. The tsunami impact was focused on Gumbet Bay on the southern coast of Bodrum with a maximum runup of 1.9 m. More considerable tsunami inundation was observed in several streambeds in the small bays, reaching 280 m. The inundation was limited only to the eastern part of the Kos Island, where the amphora-shaped bay of the Kos Port with a narrow entrance was the worst-hit area on the island. Both events showed highly localized tsunami effects with runup heights less than 5 m and first waves arriving at the nearest coast within minutes. The tsunami impact was the highest in the last event, with larger runup and inundation causing extensive loss of properties, damage to marine vessels, and a casualty. It was fortunate that this event occurred during a

pandemic and in autumn, i.e., it could have caused a significant number of injured and casualties if it had occurred during the regular summer season, considering beaches of the Aegean Sea during summer times. The observed increase in the tsunami awareness in the affected coastal areas, where it was deficient during the 2017 Bodrum-Kos event (Arikawa et al. 2017; Dogan et al. 2019), is another important finding for future social preparedness.

Acknowledgements

The authors acknowledge Yüksel Proje International Co. for significant and invaluable support, which enabled the field survey to be quick, secure, safe, and effective under pandemic conditions. The authors also acknowledge EMAY International Engineering Co. for considerable support to the expenses for the effective survey. Acknowledgements are extended to several institutions and numerous individuals for their supports at different phases of post-tsunami field survey works; the institutions and/or entities are

TÜBİTAK (Project No: 119Y419 and Project No: 5200101), METU, Yıldız Technical University, Kocaeli University, İstanbul Metropolitan Municipality, Dokuz Eylül University, İzmir Metropolitan Municipality, Çeşme Municipality, Seferihisar Municipality, and Dolfen Consultancy and Engineering Company. The distinguished individuals are Dr. Nikos Kalligeris from National Observatory of Athens, General Manager of Sığacık Teos Marina Mr. Faruk Günlü and Technical Director of Sığacık Teos Marina Mr. Özgür Uğan, General Manager of Port Alaçatı Marina Ms. Deniz Şahin, General Manager of Çeşme Marina Mr. Can Akalkan, Dr. Hasan Gökhan Güler, Civil Engineer MSc. Cem Bingöl, Civil Engineer MSc. Mehmet Sedat Gözlet, Geomatic Engineers Özgür Şahin Sarı and Seçkin Demirel, Geology Engineer Evrens Yapar and Geophysical Engineer MSc. Evrim Yavuz, Civil Engineer Yurttabir Özel, Mapping Technicians Mr. Erhan Yükselen and Mr. Ömer Mede. The eyewitnesses, Temel Okyar, Mehmet Ali Okyar, Nejat Demirkıran, Aydın Tunca, Mehmet Yarar, Zuhul Karabey, Mustafa Gül, Cengiz Özkan, are also acknowledged for their close cooperation.

Funding

Yüksel Proje International Co. provided significant and invaluable cash support and paid a considerable amount of survey and travel/accommodation expenses of the METU team members. EMAY

International Engineering Co. provided considerable support to the survey expenses. The travel expenses of Yalcın Yuksel and Cihan Şahin are covered by TÜBİTAK Project No: 5200101. TÜBİTAK Project No: 119Y419 partly supported the field expenses. In-kind support of Çeşme and Seferihisar municipalities to perform the measurements are other indirect funding to the survey.

Data Availability

The preliminary results of the first field survey (rapid survey on the 2 days after the earthquake) were published as a preliminary report (http://www.tsunami-ege.com/20201031_samos_izmir_tsunami_report.pdf and <https://drive.google.com/file/d/1HzVFjMsZ5zei2UTAoIdrcWFtPpzGr8U9/view?usp=sharing>) to share the field observations with the related global research community. The preliminary report's data have been updated with accurate measurements and detailed interpretations of eyewitness interviews obtained in the next field surveys and presented comprehensively in this paper.

Declaration

Conflict of interest The authors have no conflicts of interest.

Appendix 1

See Table 1.

Table 1

Focal parameters of the 30 October 2020 (12:51 UTC) Samos Island–İzmir earthquake and its aftershocks for $M \geq 4.0$

Date (D.M.Y)	UTC (h:min)	M_w	Depth (km)	Latitude (° N)	Longitude (° E)	Az. (°)	Dip (°)	Rake (°)	Ref
30.10.2020	12:51	6.6	16.5	37.8881	26.7770	95	43	−87	1
30.10.2020	12:53	4.7 ^a	7.1	37.8406	26.7995	93	60	−91	1
30.10.2020	12:58	4.2 ^a	7.0	37.8751	26.8986	96	53	−86	1
30.10.2020	13:01	4.0 ^a	6.8	37.8118	26.9185	97	34	−85	1
30.10.2020	13:29	4.2	7.3	37.9880	27.0716	82	53	−107	1
30.10.2020	14:00	4.8	3.4	37.8520	26.8216	111	58	−72	1
30.10.2020	14:06	4.2	7.1	37.8393	26.9850	90	45	−106	1
30.10.2020	15:46	4.0	11.0	37.8088	26.7125	91	51	−89	2
30.10.2020	16:14	5.1	7.7	37.8331	26.8690	103	45	−85	1
30.10.2020	16:19	4.4	7.0	37.8388	26.8780	97	41	−85	1
30.10.2020	21:35	4.0	13.0	37.8339	26.4862	303	60	−80	2

Table 1 *continued*

Date (D.M.Y)	UTC (h:min)	M_w	Depth (km)	Latitude (° N)	Longitude (° E)	Az. (°)	Dip (°)	Rake (°)	Ref
31.10.2020	00:05	4.0	8.0	37.8490	26.8119	119	47	-116	2
31.10.2020	02:40	4.2	16.0	37.8936	26.4855	95	57	-97	2
31.10.2020	03:10	4.1	8.0	37.8211	26.8831	91	42	-77	2
31.10.2020	06:31	5.0	7.3	37.8701	26.8303	271	52	-98	1
31.10.2020	09:47	4.0	13.0	37.9264	26.4860	95	60	-93	2
31.10.2020	05:42	4.4	12.0	37.8785	26.4579	95	42	-91	2
01.11.2020	08:05	4.2	12.0	37.9203	26.9379	89	39	-111	2
01.11.2020	08:33	4.4	11.0	37.8146	26.8477	297	74	-61	2
02.11.2020	12:58	4.0	11.0	37.8934	26.8408	109	33	-105	2
02.11.2020	21:16	4.3	13.0	37.8585	26.4478	95	65	-97	2
03.11.2020	21:35	4.0	13.0	37.8602	26.4594	260	33	-109	2
09.11.2020	21:30	4.1	10.0	37.8729	27.0078	271	54	-97	2
11.11.2020	07:49	4.3	12.0	37.8418	26.9433	92	51	-98	2

^aLocal magnitude (ML), Ref-1: AFAD (2020)—<http://deprem.afad.gov.tr>, Ref-2: NOA (2020)—<http://bbnet.gein.noa.gr>

Appendix 2

See Table 2.

Table 2

Summary of the field survey measurements

Locality	Point ID	Latitude (° N)	Longitude (° E)	Measurement (m)	Type	Inundation distance (m)	Notes
Alaçatı	AL1	38.2556	26.3833	1.0	T	–	
	AL2	38.2559	26.3820	1.0	R	73	Alaçatı Fishery Port, inundation limit
	AL3	38.2530	26.3839	1.0	T	–	
	AL4	38.2525	26.3849	1.2	T	–	
	AL5	38.2520	26.3844	0.9	R	73	Port Alaçatı, inundation limit
	AL6	38.2635	26.3730	1.7	other	–	Water level increase in the manmade channel-like port, Port Alaçatı houses
	AL7	38.2632	26.3765	1.7	other	–	Water level increase in the manmade channel-like port, Port Alaçatı houses
	AL8	38.2657	26.3775	–	–	1160	A boat was dragged up to this point
	AL9	38.2769	26.3927	–	–	2490	Maximum tsunami penetration among all surveyed locations at Alaçatı Azmak stream
Zeytineli	Z1	38.1973	26.4930	0.6	R	270	Inundation limit
	Z2	38.1964	26.4924	1.1	T		
	Z3	38.1959	26.4901	1.9	T		
	Z4	38.1959	26.4903	1.5	F		
	Z5	38.1960	26.4886	1.9	F		
	Z6	38.1951	26.4919	2.4	T		
	Z7	38.1948	26.4920	2.3	T		
	Z8	38.1974	26.4899	0.7	Other		Zeytineli Azmak bridge, water overflowed the bridge at that elevation
	Z9	38.2009	26.4933	0.6	R	710	
	Z10	38.2014	26.4936	0.5	R	760	Inundation limit
Demircili	D1	38.2116	26.6769	–	–	45	Beachside, only small inundation
	D2	38.2075	26.6864	1.0	Other		~ 1.00 water level increase inside the harbor, the sea receded to 1.80 m depth
	D3	38.2104	26.6944	0.7	R	15	

Table 2 continued

Locality	Point ID	Latitude (° N)	Longitude (° E)	Measurement (m)	Type	Inundation distance (m)	Notes
Altınköy	ALT1	38.2135	26.7220	–	–	230	Inundation limit at the beachside Tsunami penetration along the streambed
	ALT2	38.2155	26.7214	0.2	F	600	
Sığacık	S1	38.1912	26.7832	2.1	T		
	S2	38.1912	26.7844	1.5	T		
	S3	38.1911	26.7845	1.6	T		
	S4	38.1914	26.7851	1.5	T		
	S5	38.1928	26.7853	1.5	T		
	S6	38.1924	26.7862	1.0	T		
	S7	38.1941	26.7841	2.1	T		
	S8	38.1951	26.7853	2.2	T		
	S9	38.1955	26.7871	1.8	T		
	S10	38.1952	26.7872	0.7	T		
	S11	38.1961	26.7877	2.0	T		
	S12	38.1959	26.7885	–	–	140	A boat was dragged to this point from the shore
	S13	38.1958	26.7884	2.0	T		
	S14	38.1958	26.7901	1.6	R		
	S15	38.1984	26.7907	2.0	T		
	S16	38.1981	26.7909	1.8	T		
	S17	38.1983	26.7918	2.0	T		
	S18	38.1986	26.7930	1.4	R	360	
	S19	38.1992	26.7929	1.4	R	410	Maximum inundation in Sığacık
	S20	38.2012	26.7857	1.9	T		
	S21	38.2015	26.7856	1.9	R		
	S22	38.1915	26.7850	0.9	T		
	S23	38.1907	26.7830	1.2	T		
	S24	38.1912	26.7847	1.4	T		
	S25	38.1912	26.7849	1.6	T		
	S26	38.1912	26.7857	1.0	T		
	S27	38.1918	26.7863	1.3	T		
	S28	38.1919	26.7867	1.3	R		
	S29	38.1926	26.7864	1.4	R		
	S30	38.1910	26.7873	1.8	R		
	S31	38.1935	26.7861	1.3	T		
	S32	38.1940	26.7856	1.3	T		
	S33	38.1941	26.7853	1.4	T		
	S34	38.1942	26.7848	1.3	T		
	S35	38.1943	26.7847	1.4	T		
	S36	38.1951	26.7854	2.3	T		Maximum tsunami height among all surveyed locations
S37	38.1954	26.7856	1.8	T			
S38	38.1952	26.7862	1.9	T			
S39	38.1956	26.7876	1.7	T			
S40	38.1956	26.7881	1.2	T			
S41	38.2039	26.7802	1.5	R			
S42	38.1916	26.7845	0.8	F			
S43	38.1918	26.7838	0.6	F			
S44	38.1956	26.7874	0.9	F			
S45	38.1956	26.7884	0.6	F			
S46	38.1950	26.7866	0.4	F			
S47	38.1949	26.7861	0.4	F			
S48	38.2013	26.7860	1.5	F			

Table 2 continued

Locality	Point ID	Latitude (° N)	Longitude (° E)	Measurement (m)	Type	Inundation distance (m)	Notes
Akarca	A1	38.1645	26.8148	1.9	Other		Splash height Ground elevation 0.89 m
	A2	38.1644	26.8150	2.5	T		
	A3	38.1645	26.8152	–	–	55	A car was dragged to this point from the shore
	A4	38.1645	26.8154	2.4	T		
	A5	38.1651	26.8156	3.8	R	91	Maximum runup among all surveyed locations, inundation limit
	A6	38.1659	26.8148	–	–	90	A boat was dragged to this point from the shore
	A7	38.1682	26.8135	1.1	T		
	A8	38.1683	26.8135	1.0	R	290	Inundation limit
	A9	38.1667	26.8122	1.5	T		
	A10	38.1668	26.8118	1.1	T		
	A11	38.1665	26.8112	2.0	T		
	A12	38.1665	26.8107	2.1	T		
	A13	38.1680	26.8079	1.2	R	80	
	A14	38.1681	26.8112	0.9	R	250	Inundation limit
	A15	38.1641	26.8149	0.5	F	40	
	A16	38.1675	26.8092	1.5	T		
	A17	38.16693	26.8092	1.6	T		
	A18	38.1663	26.8092	2.0	T		
	A19	38.1666	26.8092	1.8	T		
	A20	38.1671	26.8091	1.9	T		
	A21	38.1672	26.8093	2.3	T		
	A22	38.1681	26.8092	1.2	R		
	A23	38.1656	26.8138	2.4	T		
	A24	38.1657	26.8137	2.9	T		
	A25	38.1667	26.8149	1.8	T		
	A26	38.1669	26.8151	1.8	T		
	A27	38.1673	26.8153	1.5	R		
	A28	38.1673	26.8154	1.6	R		
	A29	38.1671	26.8151	1.8	T		
	A30	38.1711	26.8038	–	–	20	Inundation limit
	A31	38.1647	26.8146	1.3	F		
	A32	38.1559	26.8251	0.8	F		
	A33	38.1665	26.8110	0.6	F		
	A34	38.1664	26.8120	0.8	F		
	A35	38.1681	26.8113	0.1	F	250	Inundation limit
	A36	38.1615	26.8213	0.2	F		
	A37	38.1618	26.8212	–	–	100	
	A38	38.1622	26.8215	–	–	150	Inundation limit
	A39	38.1615	26.8204	–	–	45	
	A40	38.1629	26.8190	–	–	80	Inundation limit
Tepecik	T1	38.1458	26.8201	–	–	12	Inundation limit, only sweeps
	T2	38.1390	26.8306	–	–	20	Inundation limit on the beach, only sweeps
	T3	38.1395	26.8314	–	–	120	Tsunami penetration along a small stream, Orsal Bay
	T4	38.1356	26.8331	1.5	F	–	
	T5	38.1114	26.8443	–	–	18	Inundation limit, eyewitness: 25 m sea recession

Table 2 *continued*

Locality	Point ID	Latitude (° N)	Longitude (° E)	Measurement (m)	Type	Inundation distance (m)	Notes
Gümüldür	G1	38.0757	26.9493			23	Inundation limit in front of Rafael Boutique Hotel
	G2	38.0757	26.950			15	Inundation limit, only sweeps
	G3	38.0677	26.9953				Minor damage on boats in harbor, no trace of water on objects
	G4	38.0652	26.9988	0.5	F		
	G5	38.0652	26.9992			25	Inundation limit, sweeps on a walking road
	G6	38.0577	27.0117			25	Inundation limit

R runup, *T* tsunami height, *F* flow depth, *Other* see the notes

Appendix 3

See Figs. 21 and 22.



Figure 21

Security video frames showing different stages of the tsunami motion in the Port Alaçati houses, Alaçati, Fig. 3a (38.2592° N, 26.3797° E). Timestamps are in local time (GMT + 03:00), and the earthquake time is 14:51:23 (AFAD 2020). **a** No water motion 10 min after the earthquake, **b** maximum water withdrawal (~ 1.50 m), the white boat started to move from its original location, **c** start of inundation, the white and adjacent boats, and the small berthing structures were moved and damaged, and **d** maximum water level increase (~ 1.70 m) and inundation in the region. Red and yellow ellipses show water level changes at specific locations, around the small tree over the middle breakwater and quay floor, respectively



Figure 22

Security video frames showing different stages of tsunami motion in the Kaleiçi region of Sığacık (38.1953° N, 26.7856° E). Timestamps are in local time (GMT + 03:00), and the earthquake time is 14:51:23 (AFAD 2020). **a** Start of water motion, **b** maximum sea withdrawal, **c** start of the incoming wave, **d** start of inundation, **e** significant inundation, and **f** maximum inundation in the pedestrian road. The red rectangles show (i) the boat movement in all frames due to water level change, (ii) the emerging seabed material due to sea withdrawal in the frame (**b**), and (iii) the disappeared sidewalk and bench in frames (**e**, **f**) due to inundation

Publisher's Note Springer Nature remains neutral with regard to jurisdictional claims in published maps and institutional affiliations.

REFERENCES

- AFAD (2020). Disaster and Emergency Management Authority (AFAD), Ministry of Interiors, Ankara-Turkey. <http://deprem.afad.gov.tr>.
- Anadolu Agency (2020). <https://www.aa.com.tr/tr/yasam/kismi-tsunamide-olen-kadinin-oglu-ile-torunu-yasadiklarini-anlatti/2030786#>. Accessed 03 Nov 2020.
- Aktar, M., Karabulut, H., Ozalaybey, S., & Childs, D. (2007). A conjugate strike-slip fault system within the extensional tectonics of Western Turkey. *Geophysical Journal International*, 171(3), 1363–1375. <https://doi.org/10.1111/j.1365-246X.2007.03598.x>
- Altınok, Y., Alpar, B., Ozer, N., & Gazioglu, C. (2005). 1881 and 1949 earthquakes at the Chios-Cesme Strait (Aegean Sea) and their relation to tsunamis. *Natural Hazards and Earth System Sciences*, 5, 717–725.
- Altınok, Y., Alpar, B., Ozer, N., & Vardar, H. (2011). Revision of the tsunami catalogue affecting Turkish coasts and surrounding regions. *Natural Hazards and Earth System Sciences*, 11(2), 273–291.
- Altınok, Y., & Ersoy, S. (2000). Tsunamis observed on and near the Turkish coast. *Natural Hazards*, 21, 185–205.
- Ambraseys, N. N. (1962). Data for the investigation of the seismic sea-waves in the Eastern Mediterranean. *Bulletin of the Seismological Society of America*, 52(4), 895–913.
- Ambraseys, N., & Synolakis, C. (2010). Tsunami catalogs for the Eastern Mediterranean, revisited. *Journal of Earthquake Engineering*, 14(3), 309–330.
- Arikawa, T., Guler, H. G., & Yalciner, A. C. (2017). Comparison of human response against earthquake and tsunami. In *American Geophysical Union Fall Meeting*, December 11–15, 2017, New Orleans, USA.
- Beisel, S., Chubarov, L., Didenkulova, I., Kit, E., Levin, A., Pelinovsky, E., et al. (2009). The 1956 Greek tsunami recorded at Yafo, Israel, and its numerical modeling. *Journal of Geophysical Research Oceans*, 114, C09002. <https://doi.org/10.1029/2008JC005262>
- Bozkurt, E. (2003). Origin of NE-trending basins in western Turkey. *Geodinamica Acta*, 16, 61–81.
- Chatzipetros, A., Kiratzi, A., Sboras, S., Zouros, N., & Pavlides, S. (2013). Active faulting in the north-eastern Aegean Sea Islands. *Tectonophysics*, 597, 106–122.
- Dewey, J. F., & Şengor, A. M. C. (1979). Aegean and surrounding regions: complex multiplate and continuum tectonics in a convergent zone. *Geological Society of America Bulletin*, 90, 84–92.
- Dogan, G. G., Annunziato, A., Papadopoulos, G. A., Guler, H. G., Yalciner, A. C., Cakir, T. E., et al. (2019). The 20th July 2017 Bodrum-Kos Tsunami field survey. *Pure and Applied Geophysics*, 176, 2925–2949. <https://doi.org/10.1007/s00024-019-02151-1>
- Dominey-Howes, D. (2002). Documentary and geological records of tsunamis in the Aegean Sea region of Greece and their potential value to risk assessment and disaster management. *Natural Hazards*, 25(3), 195–224.
- Emre, Ö., Duman, T. Y., Özalp, S., Elmacı, H., Olgun, Ş., & Şaroğlu, F. (2013). *New active fault map of Turkey, Mineral Research and Exploration General Directorate (MTA)*. Ministry of Energy.
- Emre, Ö., Ozalp, S., Duman, T. Y. (2011). 1:250,000 scale active fault map series of Turkey, İzmir (NJ 35-7) Quadrangle. Serial number: 6, General Directorate of Mineral Research and Exploration, Ankara.
- Evelpidou, N., Pavlopoulos, K., Vouvalidis, K., Syrides, G., Triantaphyllou, M., Karkani, A., & Paraschou, T. (2019). Holocene palaeogeographical reconstruction and relative sea-level changes in the southeastern part of the island of Samos (Greece). *Comptes Rendus Geoscience*, 351(6), 451–460.
- Galanopoulos, A. G. (1960). Tsunamis observed on the coasts of Greece from antiquity to present time. *Annals of Geophysics*, 13(3–4), 369–386.
- Jackson, J. (1994). Active tectonics of the Aegean region. *Annual Review of Earth and Planetary Sciences*, 22(1), 239–271.
- Jackson, J. A., & McKenzie, D. (1988). Rates of active deformation in the Aegean Sea and surrounding regions. *Basin Research*, 1, 121–128.
- KOERI (2020). Kandilli Observatory and Earthquake Research Institute, Istanbul-Turkey. <http://koeri.boun.edu.tr>.
- Kuran, U., & Yalciner, A. C. (1993). Crack propagations, earthquakes and tsunamis in the vicinity of Anatolia. In S. Tinti (Ed.), *Tsunamis in the world. Advances in natural and technological hazards research* (Vol. 1, pp. 159–175). Springer. https://doi.org/10.1007/978-94-017-3620-6_13
- Minoura, K., Imamura, F., Kuran, U., Nakamura, T., Papadopoulos, G. A., Takahashi, T., & Yalciner, A. C. (2000). Discovery of Minoan tsunami deposits. *Geology*, 28(1), 59–62.
- Okal, E. A., Synolakis, C. E., Uslu, B., Kalligeris, N., & Voukouvelas, E. (2009). The 1956 earthquake and tsunami in Amorgos, Greece. *Geophysical Journal International*, 178(3), 1533–1554.
- Papadopoulos, G. A., & Chalkis, B. J. (1984). Tsunamis observed in Greece and the surrounding area from antiquity up to the present times. *Marine Geology*, 56(1–4), 309–317.
- Papadopoulos, G. A., Gràcia, E., Urgeles, R., Sallares, V., De Martini, P. M., Pantosti, D., et al. (2014). Historical and pre-historical tsunamis in the Mediterranean and its connected seas: geological signatures, generation mechanisms and coastal impacts. *Marine Geology*, 354, 81–109.
- Papadopoulos, G. A., & Pavlides, S. B. (1992). The large 1956 earthquake in the South Aegean: macroseismic field configuration, faulting, and neotectonics of Amorgos Island. *Earth and Planetary Science Letters*, 113(3), 383–396.
- Papazachos, B. C., Koutitas, C., Hatzidimitriou, P. M., Karacostas, B. G., & Papaioannou, C. A. (1985). Source and short-distance propagation of the July 9, 1956 southern Aegean tsunami. *Marine Geology*, 65(3–4), 343–351.
- Papazachos, B. C., Papadimitriou, E. E., Kiratzi, A. A., Papazachos, C. B., & Louvari, E. K. (1998). Fault plane solutions in the Aegean Sea and the surrounding area and their tectonic implication. *Bollettino Geofisica Teorica Applicata*, 39(3), 199–218.
- Ring, U., Gessner, K., & Thomson, S. (2017). Variations in fault-slip data and cooling history reveal corridor of heterogeneous backarc extension in the eastern Aegean Sea region. *Tectonophysics*, 700, 108–130.

- Tan, O., Eleftheria, E. L., Pamucçu, Z., Karakostas, V., Yörük, A., & Leptokarpoulos, K. (2014). A detailed analysis of microseismicity in Samos and Kusadasi (Eastern Aegean Sea). *Acta Geophysica*, 62(6), 1283–1309. <https://doi.org/10.2478/s11600-013-0194-1>
- Taymaz, T., Jackson, J., & McKenzie, D. (1991). Active tectonics of the north and central Aegean Sea. *Geophysical Journal International*, 106(2), 433–490. <https://doi.org/10.1111/j.1365-246X.1991.tb03906.x>
- Tepe, Ç., & Sözbilir, H. (2017). Tectonic geomorphology of the Kemalpaşa Basin and surrounding horsts, southwestern part of the Gediz Graben, Western Anatolia, Anatolia. *Geodinamica Acta*, 29(1), 70–90. <https://doi.org/10.1080/09853111.2017.1317191>
- Tinti, S., Maramai, A., & Graziani, L. (2001). A new version of the European tsunami catalogue: updating and revision. *Natural Hazards and Earth System Sciences*, 1, 255–262.
- Triantafyllou, I., Gogou, M., Mavroulis, S., Lekkas, E., Papadopoulos, G. A., & Thravalos, M. (2021). The tsunami caused by the 30 October 2020 Samos (Aegean Sea) Mw7.0 earthquake: hydrodynamic features, source properties and impact assessment from post-event field survey and video records. *Journal of Marine Science and Engineering*, 9, 68. <https://doi.org/10.3390/jmse9010068>.
- UNESCO (2014). International Tsunami Survey Team (ITST) Post-Tsunami Survey Field Guide. 2nd Edition. IOC Manuals and Guides No.37, Paris: UNESCO 2014 (English).
- Wessel, P., & Smith, W. H. (1998). New, improved version of generic mapping tools released. *Eos Transactions American Geophysical Union*, 79(47), 579–579.
- Yalciner, A. C., Kuran, U., Akyarlı, A., & Imamura, F. (1995). An investigation on the propagation of tsunamis in the Aegean Sea by mathematical modeling. In Y. Tsuchiya & N. Shuto (Eds.), *Tsunami: progress in prediction, disaster prevention and warning. Advances in natural and technological hazards research* (Vol. 4, pp. 55–70). Springer. https://doi.org/10.1007/978-94-015-8565-1_4

(Received December 21, 2020, revised March 4, 2021, accepted March 6, 2021, Published online March 22, 2021)